Fragment Screening Yields a Small-Molecule Stabilizer of 14-3-3 Dimers That Modulates Client Protein Interactions

Hendrik J. Brink,[a] Rick Riemens,[a] Stephanie Thee,[a] Berend Beishuizen,[a] Daniel da Costa Pereira,[a] Maikel Wijtmans,[a] Iwan de Esch,[a] Martine J. Smit,*[a] and Albertus H. de Boer*[a]

The development of protein-protein interaction (PPI) inhibitors has been a successful strategy in drug development. However, the identification of PPI stabilizers has proven much more challenging. Here we report a fragment-based drug screening approach using the regulatory hub-protein 14-3-3 as a platform for identifying PPI stabilizers. A homogenous time-resolved FRET assay was used to monitor stabilization of 14-3-3/peptide binding using the known interaction partner estrogen receptor alpha. Screening of an in-house fragment library identified fragment **2** (VUF15640) as a putative PPI stabilizer capable of cooperatively stabilizing 14-3-3 PPIs in a cooperative fashion with Fusicoccin-A. Mechanistically, fragment **2** appears to enhance 14-3-3 dimerization leading to increased client-protein binding. Functionally, fragment **2** enhanced potency of 14-3-3 in a cell-free system inhibiting the enzyme activity of the nitrate reductase. In conclusion, we identified a general PPI stabilizer targeting 14-3-3, which could be used as a tool compound for investigating 14-3-3 client protein interactions.

Introduction

In recent years significant advances have been made in drug discovery regarding protein-protein interaction (PPI) inhibitors targeting sites previously regarded as undruggable.[1] In contrast, the development of PPI stabilizers has proven to be much more difficult. Potential PPI stabilizers, unlike inhibitors, are required to contact both proteins on the interaction interface to function as a molecular glue, increasing the affinity, duration and stability of this complex.[2] Nonetheless, the development of PPI stabilizers is attractive as it could potentially allow for the development of cooperatively binding compounds with a higher selectivity as the targeted interaction interface is unique for each PPI complex.

A key family of proteins studied in the context of PPI stabilization is the essential scaffolding and regulatory protein family 14-3-3 found in all eukaryotes.[3] In mammalian cells, there are seven different isoforms known (α, β, γ, ε, ζ, η and θ) that are active either as monomers or as homo- and heterodimers.[4] Structurally a 14-3-3 monomer consists of nine anti-parallel alpha-helices that dimerize at the N-terminus to form a wedged-shaped protein.[5] Each monomer contains an amphipathic binding groove in which 14-3-3 can bind client proteins based on their phosphorylated motifs such as the RAF kinases B- and C-RAF.[5,6] The binding motifs recognized in client proteins are subdivided into different modes with mode-I (RSX[pS/pT]XP) and II (RXXX[pS/pT]XP) occurring anywhere in the client protein sequence, whereas mode-III (XXX[pS/pT]X-COOH) binding motifs are found at the extreme C-terminus of the client protein.[7,8] Mode I and II 14-3-3 interactions have been extensively studied, with more than 200 client proteins identified.[9,10] Mode III interactions have been less extensively studied and these interactions differ structurally from mode I and II as the C-terminus of the client protein terminates inside the 14-3-3 binding groove.[8] As a result, a cavity is formed by the surface of the 14-3-3 groove and the C-terminal amino acid of the client protein that a PPI stabilizer can target.[7]

The first example of a PPI stabilizer targeting 14-3-3/client protein interactions was the natural product Fusicoccin-A (FC-A), a diterpene glucoside isolated from the fungus *Phomopsis amygdali*.[11] FC-A was shown to target the interaction between 14-3-3 and the plant H^+-ATPase PMA2. Since the discovery of FC-A as a PPI stabilizer, several mammalian 14-3-3/FC-A targets have been identified, including the cystic fibrosis transmembrane conductance regulator (CFTR) and the stress response regulator GCN1.[12,13] Previously, we have shown in human MCF-7 breast cancer cells that FC-A targets the mode-III interaction between 14-3-3 and the nuclear transcription factor the estrogen receptor alpha (ERα).[14] FC-A stabilization of the 14-3-3/ERα interaction prevents ERα dimerization and subsequent transcriptional activity, which results in decreased cellular proliferation providing a new avenue for targeting ERα-driven breast cancer.[14]

Unlike PPI inhibitors, FC-A contacts both 14-3-3 and ERα, acting as a molecular glue to increase the affinity of the complex. Consequently, the 14-3-3 proteins provide a unique setting to study PPI stabilization. Unlike other PPI stabilizers

[a] H. J. Brink, R. Riemens, S. Thee, B. Beishuizen, D. da Costa Pereira, Dr. M. Wijtmans, Prof. I. de Esch, M. J. Smit, Dr. A. H. de Boer
Division of Medicinal Chemistry, Faculty of Sciences
Amsterdam Institute for Molecular and Life Sciences (AIMMS)
De Boelelaan 1108, 1081 HZ Amsterdam (The Netherlands)
E-mail: m.j.smit@vu.nl
ahdeboer54@gmail.com

Supporting information for this article is available on the WWW under https://doi.org/10.1002/cbic.202200178

such as Rapamycin or Tafamidis that target a fixed set of protein interactions, the 14-3-3 protein family interacts with many different client proteins providing opportunities to target and modulate PPIs in many different settings. The 14-3-3/ERα interaction complex has emerged as a novel platform for developing PPI stabilizers.[15,16]

In the present study, we set out to identify novel PPI stabilizers targeting 14-3-3 using a fragment-based screening approach. Fragment screening is an approach that is complementary to high-throughput screening and is able to efficiently sample chemical space of protein binders by using small libraries of small molecules.[17,18] Fragment approaches targeting the 14-3-3 interface with various protein interaction partners using both covalent and non-covalent fragments have been reported.[19–26] Whereas the 14-3-3/ERα interface has previously been targeted by stabilizing covalent fragments,[22] here we target the 14-3-3/ERα interaction with stabilizing non-covalent fragments. Our in-house fragment library of 1600 non-covalent fragments was screened using a homogenous time-resolved FRET assay (HTRF). Fragment **2** was identified as a hit and validated in an orthogonal fluorescent polarization assay (FP). We show that fragment **2** acts cooperatively with FC-A to stabilize 14-3-3 PPIs. HTRF and protein cross-linking data suggest that fragment **2** stabilizes 14-3-3 dimers. The binding of fragment **2** to 14-3-3 translated into a functional effect as fragment **2** could enhance the potency of 14-3-3 in an enzyme assay inhibiting the plant nitrate reductase.

Results and Discussion

The 14-3-3/ERα HTRF assay setup

This study employed a fragment screening approach to identify putative stabilizers of the 14-3-3/ERα interaction complex. Our in-house fragment library[27,28] was screened using an HTRF readout in which 14-3-3 protein binding to an ERα peptide was monitored (Figure 1A). For this screen, we used recombinant N-terminally GST-tagged 14-3-3η, which was labeled with a europium cryptate conjugated anti-GST antibody. The binding of an N-terminally biotinylated phosphorylated ER-alpha peptide (Bio-KYYITGEAEGFPA**pT**^{594}V; ERα-TV) labeled with streptavidin-XL665 to 14-3-3η was evaluated (Figure 1B). Titrating increasing amounts of ERα-TV peptide to GST-14-3-3η increased the peptide/14-3-3η binding, observed as an increase in the FRET-ratio (Figure 1B). Moreover, the addition of 10 μM of the known interaction stabilizer FC-A (Figure 1E) induced a leftward shift of the concentration-response curve, indicative of an enhanced affinity of the peptide for 14-3-3η (Figure 1B). These data validate the HTRF assay as a tool for detecting PPI stabilizers of the ERα/14-3-3 complex *in vitro*.

Primary screening of 1600 fragments against the 14-3-3/ERα interaction

In total, 1600 fragments were screened at 200 μM in a 384-well format using the HTRF assay in a single-point format (Figure 1C & Figure S1A–E). Z' factors were determined using three control conditions per plate, and amounted to $\geq$0.79 for individual plates, indicating a high sensitivity for detecting 14-3-3/ER-alpha stabilizers.[29] Hits were characterized as fragments with a Z-score of 10 or greater (Figure 1C). The initial screen yielded 133 fragments with Z-scores $>$10; of these 23 were dropped for excessively exceeding the Z-score of the reference compound FC-A. Another 15 compounds were excluded due to solubility issues at assay concentrations. Next, the following selection criteria were applied: putative hits should stabilize the 14-3-3/ERα-pTV interaction whilst not affecting the HTRF signal in the absence of 14-3-3 and the ERα-pTV peptide. A total of 95 fragments were tested in a single point format at 200 μM, of which only one fragment met the selection criteria and was therefore selected for further analysis (Figure 1D, S2C & H).

The fragment had been synthesized about a decade before our current research commenced and had been stored since at room temperature and protected from light. Its recorded structure was **1**, but structure validation using NMR spectroscopy comparing to a commercial sample of **1**, as well as MS analysis, did not support this, but instead suggested the fragment being of structure **2** (Figure 1F). To confirm its identity, fragment **2** was newly synthesized by an indirect reductive amination between racemic quinuclidin-3-amine dihydrochloride and quinuclidin-3-one hydrochloride. The chemical analyses (NMR, LC–MS) of newly synthesized fragment **2** as well as its biochemical properties as measured by the two orthogonal 14-3-3 assays (*vide supra*) matched those of the initial hit fragment. We therefore used this new batch of fragment **2** for our subsequent work. Control fragment **3** was designed to lack one terminal basic center compared to fragment **2** (Figure 1F). It was prepared analogously to **2** but with bicyclo[2.2.2]octan-2-one. We were unable to unequivocally assign the stereochemical composition of fragments **2** and **3**. To the best of our knowledge (Reaxys search engine executed December 2021), neither fragment **2** nor fragment **3** have been disclosed in the peer-reviewed and patent literature before. Noteworthy, with all atoms being sp^3-hybridised, these fragments have an unusually high three-dimensionality and their study will align well with ongoing investigations on 3D fragments in the field.[30]

Concentration-response curves with selected fragments

The stabilizing effect of the selected fragment **2** on the ERα-pTV/14-3-3η interaction was further characterized and compared to the effect of FC-A. The ERα-pTV/14-3-3η interaction was stabilized in a concentration-dependent manner by both FC-A and fragment **2** with pEC_{50} values of 5.8 and 3.5 respectively (Figure 2A, Table S3). Notably, increases in the

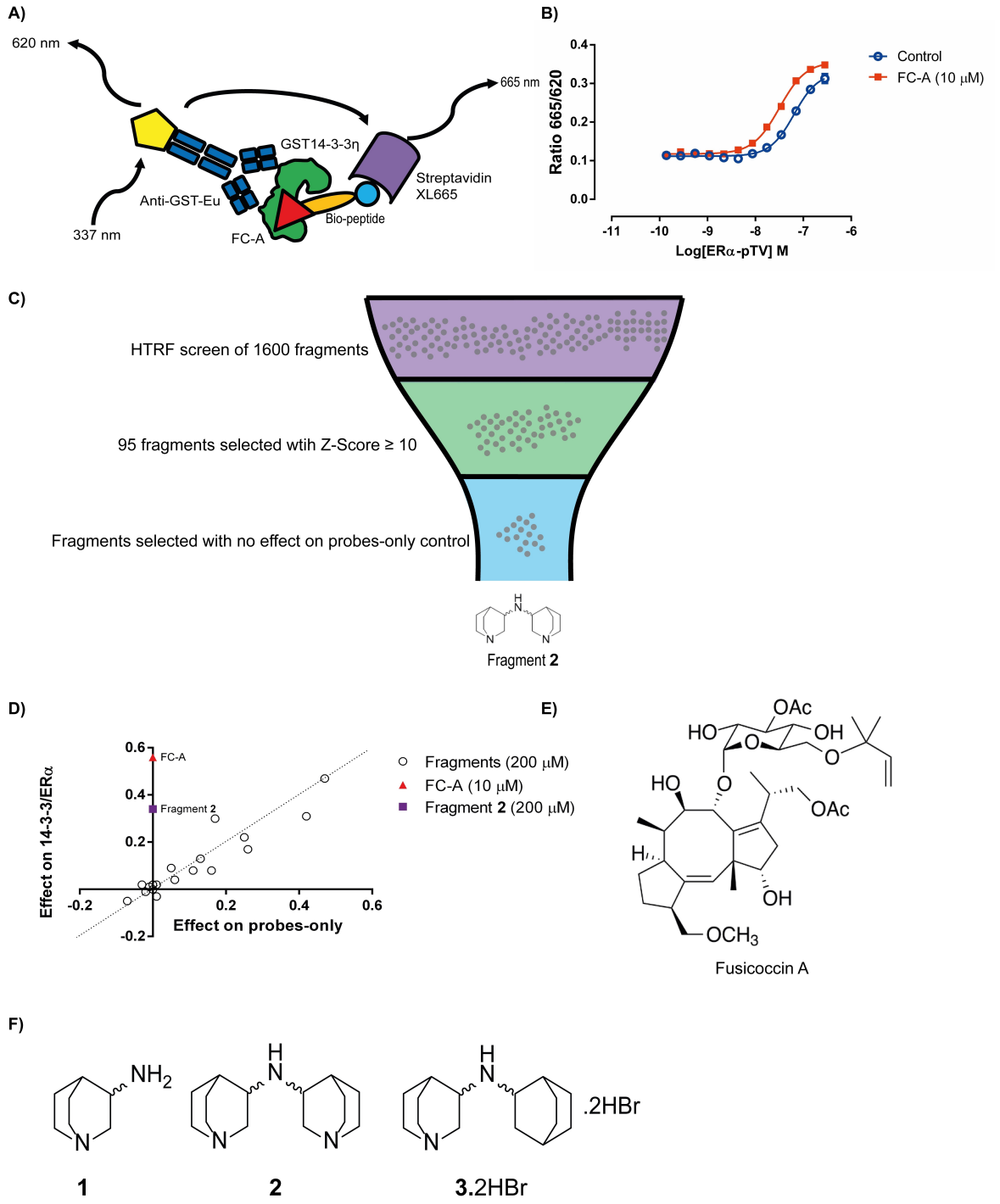

Figure 1. Fragment library screen for PPI stabilizers of the ERα/14-3-3 interaction complex. A) Cartoon illustrating our homogeneous time resolved FRET (HTRF) assay in which an N-terminally GST tagged 14-3-3η is targeted with an anti-GST europium (Eu) cryptate labelled monoclonal antibody and ERα peptides used are N-terminally biotinylated and labelled with streptavidin conjugated to XL665. Europium is excited at a wavelength 337 nm resulting in emission at a wavelength of 620 nm. If the 14-3-3 interacts with the ERα peptide, resonance energy transfer can occur resulting in excitation and emission of XL665 at a wavelength of 665 nm. B) ERα-pTV peptide binding to 10 nM GST14-3-3η in the absence (blue) or presence of 10 μM Fusicoccin (FC-A, red). C) Overview of HTRF based fragment library screen. D) XY plots of fragments selected for further validation in which the effect on the 14-3-3/ERα-pTV interaction complex is plotted against the effect on only the HTRF probes in absence of the protein or peptides. E) Structure of FC-A. F) Structure of compound **1**–**3**. Representative figures are shown of n = 3 experiments; data are shown as mean ± SD.

HTRF ratio at saturating concentrations were significantly higher for fragment **2** than FC-A ($P = 0.0016$). Commercial **1** was also tested as a negative control, but it did not display any stabilizing effect in our HTRF assay, confirming the reassignment in the structure of the initial hit (*vide supra*)

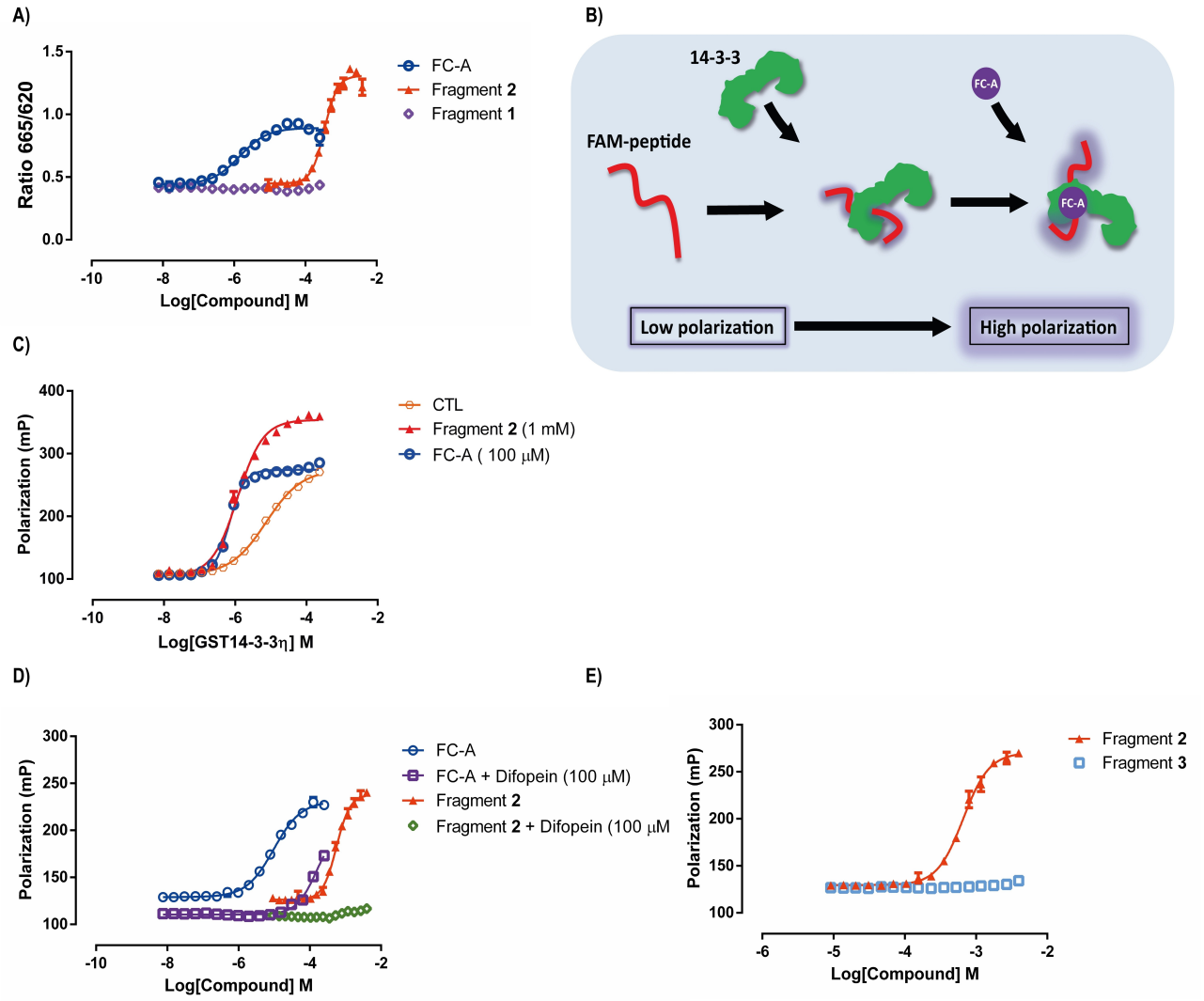

Figure 2. Validating fragment **2** in HTRF and orthogonal fluorescent polarization assay. A) Concentration-response curves of FC-A, fragment **2** and compound **1** generated with the HTRF assay with 50 nM ERα-pTV peptide and 10 nM GST14-3-3η. B) Cartoon of fluorescent polarization assay. C) GST14-3-3η titration against fixed saturating concentrations of FC-A (100 μM), fragment **2** (1 mM) or buffer control (CTL) in combination with 100 nM FAM-ERα-pTV in fluorescent polarization assay. D) Concentration-response curves of FC-A and fragment **2** generated in the fluorescent polarization assay using 100 nM of the FAM – ERα-pTV peptide and 1.5 μM of GST14-3-3η with or without a fixed 100 μM of the non-labelled 14-3-3 inhibitor peptide difopein. E) Concentration-response curves of fragment **2** and fragment **3** generated in the fluorescent polarization assay using 100 nM of FAM-ERα-pTV peptide and 1.5 μM of GST14-3-3η. Representative figures are presented of n = 3 experiments. Data are shown as mean ± SD.

and indicating that both quinuclidine rings are needed for activity (Figure 2A).

Orthogonal fluorescent polarization assay

A fluorescent polarization (FP) setup was used as an orthogonal assay to further validate fragment **2** as a putative stabilizer of the 14-3-3/ERα interaction complex (Figure 2B). In this setup, the ERα-pTV peptide is N-terminally labeled with fluorescein (FAM). The binding of GST14-3-3η to the FAM-ERα-pTV peptide increases the fluorescent polarization values over that of the free peptide (Figure 2B). Increases in polarization levels detected in the presence of a molecule such as FC-A is a measure of protein/peptide stabilization. First, GST14-3-3η was titrated into a solution of FAM-ERα-pTV combined with saturating levels of FC-A (100 μM), fragment **2** (1 mM) or a buffer-control (Figure 2C). The pEC_{50} value of the GST14-3-3η binding to FAM-ERα-pTV was 5.13 ± 0.006 (mean ± SEM) in the absence of any compound. The pEC_{50} value was enhanced by fragment **2** to 5.92 ± 0.015 due to the addition of fragment **2** or to 6.16 ± 0.013 in the presence of FC-A (Table S4). Interestingly, the max mP values observed for fragment **2** were significantly higher than that of FC-A in these experiments; 360 ± 0.86 mP compared to 284 ± 0.58 mP ($p < 0.0001$) respectively (Figure 2C). Next, we investigated the concentration-dependent effect of FC-A and fragment **2** on the GST14-3-3η/FAM-ERα-pTV interaction. FC-A and fragment **2** enhanced the observed protein/peptide interaction with pEC_{50} values of 5.23 and 3.22,

respectively, comparable to the HTRF assay (Figure 2D; Table S4).

Next, we sought to establish that the observed effect of fragment **2** in our FP assay was specific for FAM-ERα-pTV binding to 14-3-3 and not the result of fragment **2** exerting effects on FAM-ERα-pTV fluorescence. To this end, we used difopein, a non-labeled bivalent peptide that competes for ERα peptide binding as it binds 14-3-3 dimers in both grooves in a phosphorylation-independent manner.[31] The stabilizing effect exerted by both FC-A and fragment **2** could be inhibited in the presence of a fixed concentration of difopein, indicating that the observed effects are ERα-pTV peptide dependent (Figure 2D). The measured FP baseline in the case of difopein is lower than that of FC-A or fragment **2** only as difopein is capable of almost completely displacing the FAM-ERα-pTV peptide. Finally, the effect of fragment **2** on FAM-ERα-pTV binding to GST14-3-3η was compared to fragment **3**, an analog lacking one terminal basic center (Figure 1F). In contrast to fragment **2**, fragment **3** did not stabilize the ERα/14-3-3 interaction (Figure 2E).

In conclusion, fragment **2** was validated to stabilize the ERα/14-3-3 interaction in HTRF and FP assays, with a higher efficacy but lower potency than FC-A.

Fragment 2 functions additively with FC-A

We next investigated whether the combination of fragment **2** and FC-A had an additive or competitive effect on the GST14-3-3η/FAM-ERα-pTV interaction. Fragment **2** concentration-response curves were generated in the absence and presence of a saturating concentration of FC-A (Figure 3A). The obtained pEC_{50} values for the FC-A -response curve were 5.12, 3.22 for fragment **2** and 3.47 for the combination of fragment **2** plus a fixed 100 μM of FC-A (Figure 3A; Table S4). Strikingly, fragment **2** induces an additive concentration-dependent effect in the presence of a saturating concentration FC-A with a minimal

A)

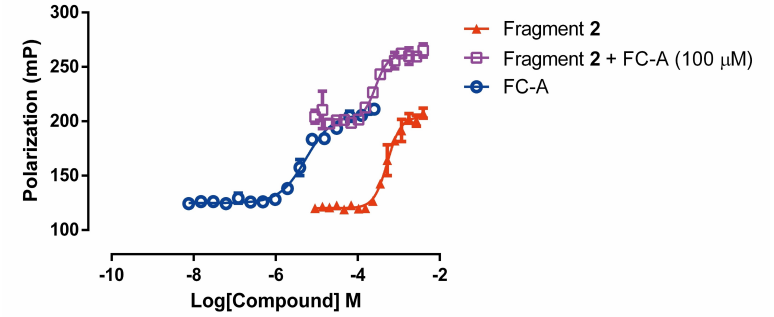

B)

ERα-pTV	Bio	K	Y	Y	I	T	G	E	A	E	G	F	P	A	pT^{594}	V	-
ERα-pTF	Bio	K	Y	Y	I	T	G	E	A	E	G	F	P	A	pT^{594}	F	-
ERα-pTVF	Bio	K	Y	Y	I	T	G	E	A	E	G	F	P	A	pT^{594}	V	F
ERα-P592N	Bio	K	Y	Y	I	T	G	E	A	E	G	F	N	A	pT^{594}	V	-
ERα-Condor	Bio	F	Y	I	N	S	K	E	E	E	N	M	Q	N	pT^{585}	I	-

C)

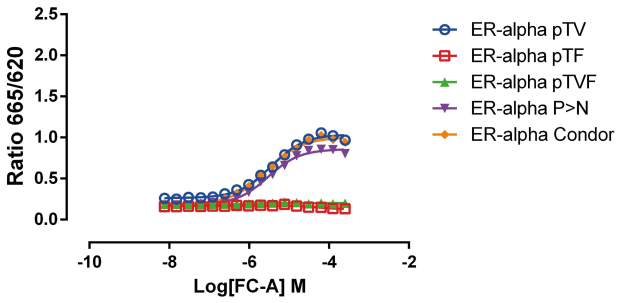

D)

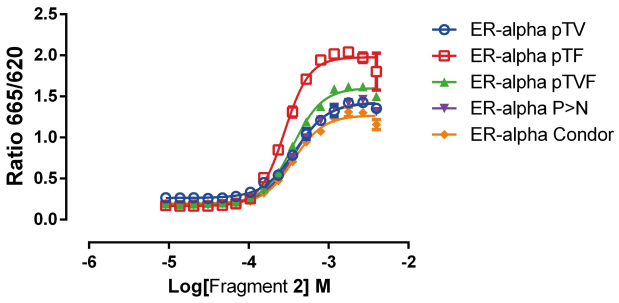

Figure 3. Testing of fragment **2** in combination with FC-A. A) Concentration-response curves generated with FC-A, fragment **2** or fragment **2** combined with a fixed 100 μM concentration of **FC-A** in the presence of 100 nM of the FAM-ERα-pTV and 1.5 μM of GST14-3-3η. B) Table showing the name and sequence of five different ERα peptides used. Amino acid classes color coded; positively charged (blue), negatively charged (red) hydrophobic side chains (green), polar uncharged sides chains (purple) and phosphorylated residue (yellow). C, D) Concentration-response curves of FC-A and fragment **2** against 50 nM of the different peptides listed in the table above and 10 nM of GST14-3-3η. Representative figures are presented of n = 3 experiments. Data are shown as mean ± SD.

difference in potency. This indicates that fragment **2** and FC-A can bind simultaneously in a non-competitive manner to stabilize the GST14-3-3η/FAM-ERα-pTV interaction. As such, these findings raise the question of whether fragment **2** targets the canonical FC-A pocket or another allosteric site of the ERα/14-3-3 interaction complex as no competition was observed with FC-A.

Because fragment **2** was shown to enhance GST14-3-3η/FAM-ERα-pTV binding in an additive manner when combined with FC-A (Figure 3A), we next explored whether fragment **2** targets the canonical FC-A pocket formed by the 14-3-3 groove and the ERα peptide or another region of the 14-3-3 protein. To this end, we generated fragment **2** concentration-response curves against modified peptides in which either the C-terminal Valine was replaced by a Phenylalanine, an amino acid not compatible with FC-A binding (ERα-pTV→ERα-pTF) or where the FC-A pocket was occluded by extending the peptide into the FC-A pocket (ERα-pTV→ERα-pTVF; Figure 3B). In addition, two peptides were included that retained susceptibility to FC-A mediated stabilization, where the amino acid sequence upstream of the phosphorylation site forming the rest of the interaction interface differed markedly from that of the WT peptide. Namely, a peptide (ERα-P592 N; KYYITGEAEGFNA**pT**^{594}V) in which Pro592 had been substituted for asparagine or a C-terminal peptide of the ERα derived from the Californian condor (ERα-Condor; FYINSKEEENMQN**pT**^{585}I) (Figure 3B). As expected, FC-A was capable of stabilizing the interactions between the ERα-pTV, ERα-P592 N and ERα-Condor peptides but not that of the ERα-TF or ERα-TVF peptides, in which the FC-A pocket had been perturbed (Figure 3C; Table S3). In contrast, fragment **2** stabilized the interaction between all ERα peptides with similar pEC_{50} values ranging from 3.39 to 3.5 (Figure 3D; Table S3). Similar to what was observed for the ERα-pTV peptide, the absolute HTRF ratio was significantly higher for fragment **2** at saturating levels in combination with the ERα-P592 N and ERα-Condor than for FC-A ($p < 0.0001$). The obtained results suggest that firstly fragment **2**, unlike FC-A, can enhance ERα/14-3-3 binding in a setting where the FC-A pocket has either been altered or occluded. Secondly, changes in the rest of the ERα/14-3-3 interface do not change the stabilizing effect observed for fragment **2** on ERα/14-3-3 binding.

Fragment 2 stabilizes 14-3-3 dimerization

We set out to determine the mechanism of action by which fragment **2** stabilizes the interaction between 14-3-3 and the ERα peptide. Our FP and HTRF data suggest that fragment **2** does not target the canonical FC-A pocket and does increase the maximally observed polarization level compared to FC-A. This indicates that fragment **2** targets an allosteric site in 14-3-3, altering dimer formation and/or inducing conformational changes in the protein. As such, we formulated a hypothesis that explains the aforementioned findings, namely; fragment **2** affects 14-3-3 dimerization and subsequently induces a conformational change that results in enhanced peptide binding. It has, for example, been well documented that as a result of conformational changes, the 14-3-3 binding groove can adopt a more open or closed conformation, facilitating binding to a large subset of proteins of varying sizes and sequences.[5]

To test the hypothesis that fragment **2** affects dimer (con)formation, we used a modified HTRF assay. We produced and purified two recombinant 14-3-3 isoforms, 14-3-3η and 14-3-3γ, which were labeled with different tags, GST and His respectively. In an HTRF assay GST-14-3-3η monomers can bind to antibodies labeled with the HTRF donor Europium and His-14-3-3γ monomers can bind to the acceptor streptavidin-XL665 (Figure 4A). It has been shown for both 14-3-3η and 14-3-3γ that monomer swapping can occur between homodimers of these isoforms resulting in heterodimers.[5,32] If, upon mixing of the two isoforms no heterodimers (GST-14-3-3η/His-14-3-3γ) are formed, the HTRF signal will be low as the donor and acceptor are not in close proximity. However, the dimer/monomer equilibrium is dynamic and heterodimers can form (to different degrees in an isoform-dependent manner).[5] If that happens, a GST-14-3-3η/His-14-3-3γ heterodimer will yield an HTRF signal as now the donor and acceptor are brought in close proximity. Figure 4B shows that FC-A and fragment **3** do not affect the basal HTRF signal in an assay where both GST-14-3-3η and His-14-3-3γ are present. However, titration with fragment **2** resulted in a concentration-dependent increase in the HTRF signal with a pEC_{50} value of 3.62 ± 0.02 (Figure 4B). This effect of fragment **2** is independent from the binding of a client peptide, as shown by the absence of an effect of a fixed concentration of the ERα-pTV peptide (Figure 4B). From these results, we conclude that the effect of fragment **2** on the binding of phospho-peptides to 14-3-3 is driven by a direct interaction with 14-3-3 and not with the binding peptides. This corroborates the conclusion drawn from Figure 3D, namely that the enhanced binding of phospho-peptides to 14-3-3 in the presence of fragment **2** is sequence-independent.

Allosteric binding (allosteric to the FC-A pocket) of fragment **2** to 14-3-3, driving a conformational change and inducing a more closed conformation of the binding groove, can explain many of the described results. However, it cannot be excluded that this allosteric binding site is at the interface of the two monomers that form a dimer as compounds have previously been reported that target this interface.[33] We used the same experimental HTRF setup as described above to address this question. Our hypothesis was that fragment **2** binds at the dimer interface (homo- or hetero) and stabilizes dimer formation. If that is the case, then a pre-incubation of: (i) (GST-14-3-3η + fragment **2**) and (His-14-3-3γ + fragment **2**) separately for 2 h, followed by mixing and addition of HTRF probes, or (ii) (GST-14-3-3η + His-14-3-3γ) for 2 h, followed by mixing and addition of fragment **2** and HTRF probes, should yield different HTRF signals (Figure 4C & D). In the first example, the homodimers are fixed by fragment **2** and no heterodimers can form upon mixing, whereas in the second example heterodimers are formed first followed by stabilization by fragment **2**. We used the same mixing schemes as a

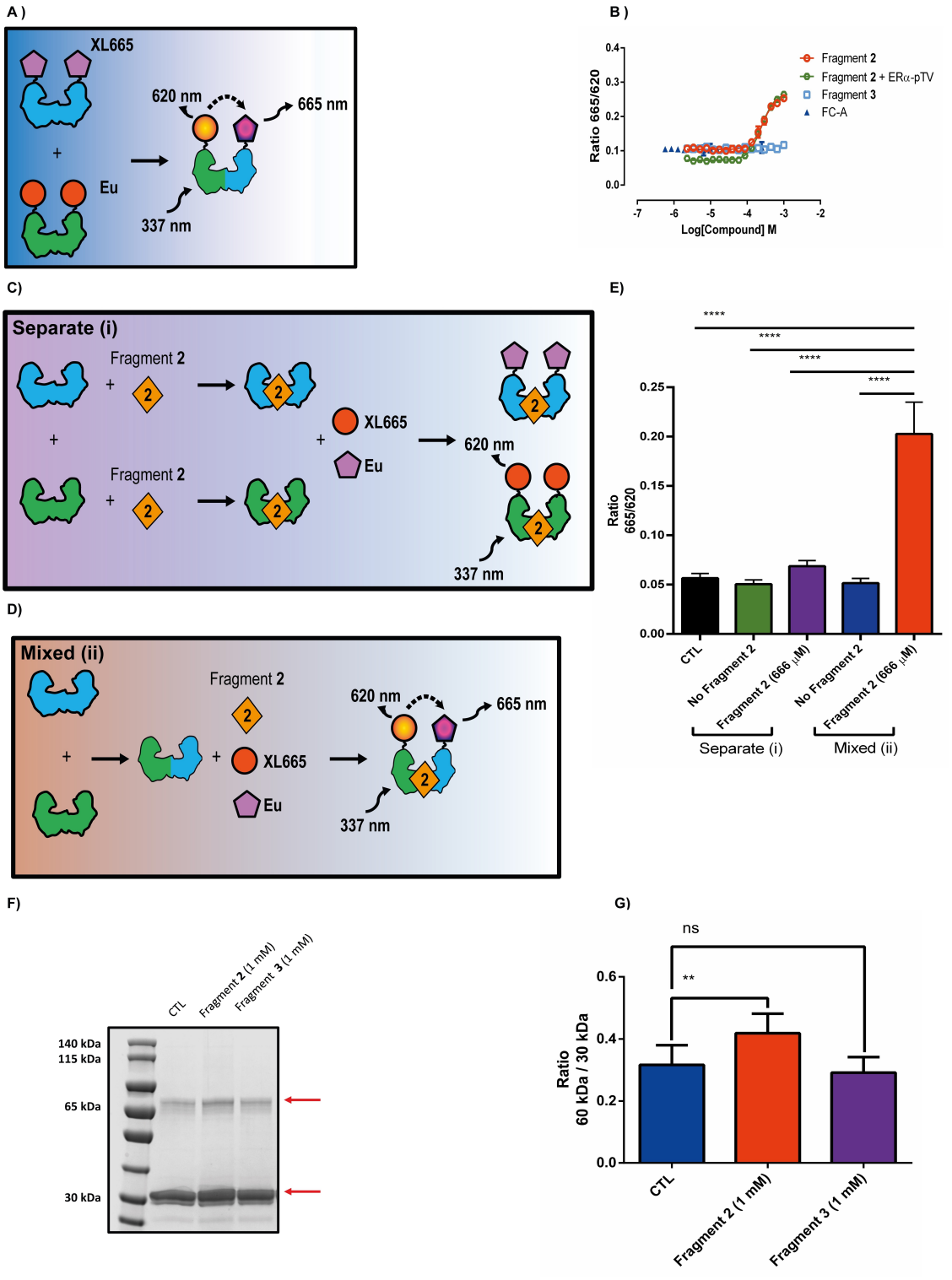

Figure 4. Testing of fragment **2** on 14-3-3/14-3-3 interactions. A) Cartoon overview of 14-3-3 interaction assay using GST14-3-3η labelled with Europium cryptate and His14-3-3γ labelled with the acceptor XL665. B) Fragment **2**, fragment **3** and FC-A concentration-response curves generated with Europium cryptate labelled GST14-3-3η and XL665 labelled His14-3-3γ. Fragment **2** curve generated in the presence and absence of 50 nM ERα-pTV peptide. A representative figure is shown of three independent experiments. C) Cartoon overview of Europium cryptate labelled GST14-3-3η (shown in green) and XL665 labelled His14-3-3γ (shown in blue) pre-incubation experiments with fragment **2** (orange diamond). In which GST14-3-3η and His14-3-3γ are pre-incubated with fragment **2** followed by the addition of HTRF probes or D) GST14-3-3η and His14-3-3γ are mixed together before the addition of fragment **2** and the HTRF probes. E) HTRF 665/620 ratios of fragment **2** pre-incubation experiments. Data are presented as the mean ± SEM of three independent experiments. Differences analyzed by one-way ANOVA ($\alpha = 0.05$, $p < 0.0001$). F) Paraformaldehyde cross-linking of His14-3-3γ in the presence of buffer (CTL), fragment **2** or fragment **3**. Samples were ran on a SDS-PAGE gel and visualized by instant blue staining. G) Quantification of the SDS-PAGE gel seen in panel F, ratios of the 65 kDa band over the 30 kDa band are shown. Differences analyzed by one-way ANOVA ($\alpha = 0.05$, $p = 0.003$). Data are presented as the mean ± SEM of three independent experiments.

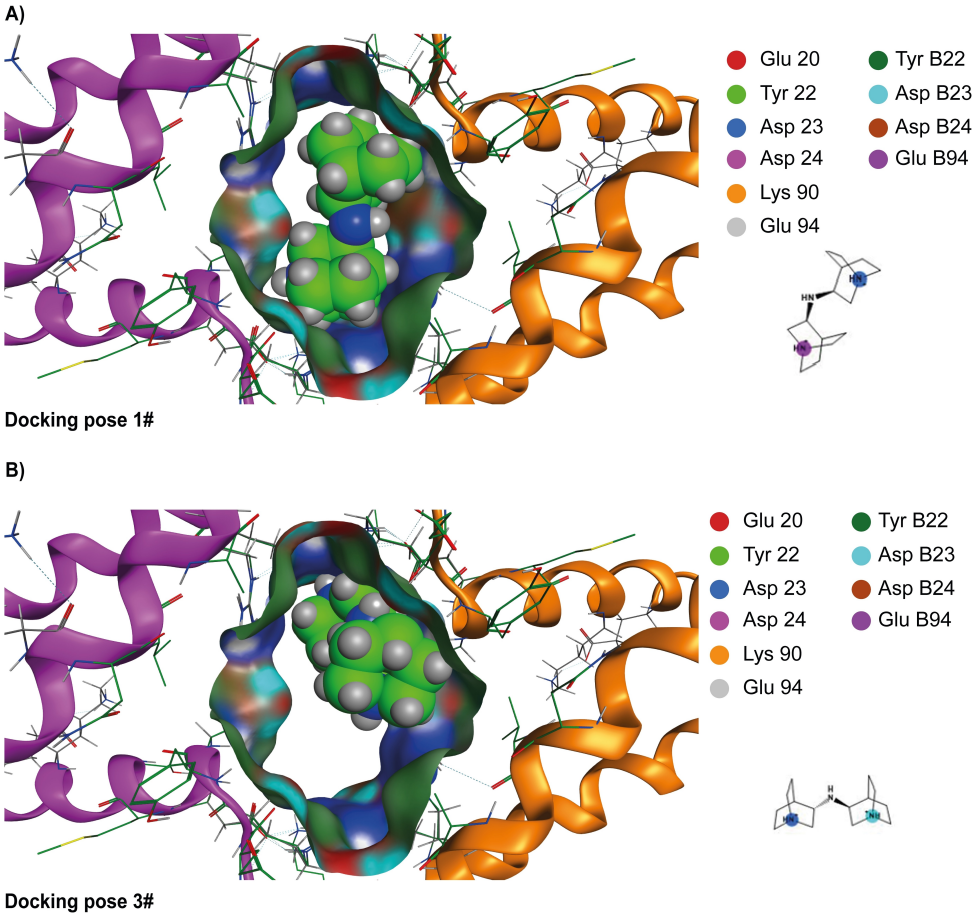

Figure 5. Molecular docking studies suggest fragment **2** can bind in the central cavity of 14-3-3. A) Docking pose 1# and B) 3# are shown in which fragment **2** (green surface structure) is docked in the central pore of 14-3-3η. The 14-3-3η dimer is represented as a stick and ribbon structure with monomers colored purple (left) and orange (right). Amino acids relevant for fragment **2** binding are color coded and shown on the right.

control, but then without fragment **2**. Figure 4E shows that even as the end composition of the solutions is the same, the resulting HTRF signal is determined by the order in which the different components are mixed. If the 14-3-3s are first exposed separately to fragment **2** and thereafter mixed, the HTRF signal only marginally increases above baseline (Figure 4E, separate). However, if both 14-3-3 isoforms are mixed (and monomer exchange can proceed), then the addition of fragment **2** induces a robust increase in the HTRF signal (Figure 4E, mixed). This result supports our hypothesis that fragment **2** does affect the formation/stabilization of dimers.

To support this conclusion, we measured the relative amount of 14-3-3 dimers in a given sample by cross-linking with paraformaldehyde (PFA) and subsequent analysis on SDS-PAGE. As the SDS-PAGE conditions are denaturing, 14-3-3 dimers dissociate and mainly run as monomers. Without cross-linking (no PFA), His14-3-3γ indeed showed a distinct band at 30 kDa corresponding to the monomeric form of the protein and a light band at approximately 65 kDa (Figure S3A). The latter was significantly increased after cross-linking with 0.2% PFA, because cross-linked monomers remain in the dimer form on SDS-PAGE (Figure S3A). If the dimer/monomer ratio is higher in a given sample, then PFA-induced cross-linking of the 14-3-3 monomers will be more efficient. After SDS-PAGE, a higher ratio of the intensity of the 65 and 30 kDa bands will reflect the relative dimerization state. Figures 4F and G show that with fragment **2** (but not with the inactive analog fragment **3**), the 65 kDa band becomes more prominent resulting in an increased 65:30 kDa ratio ($p = 0.0003$). Thus, these results confirm that fragment **2** affects 14-3-3 dimer formation independent of peptide binding.

Fragment docking

Efforts to elucidate the binding mode of fragment **2** with 14-3-3 with X-ray analysis after co-crystallization or soaking approaches failed. To illustrate the shape complementarity between fragment **2** and the 14-3-3 dimer, we used the molecular modelling package MOE (Chemical Computing Group, version 2020.09). Protein structure 7nmz.pdb[34] of 14-3-3η was protonated (pH = 7.4) and possible ligand binding sites were identified by using the Site Finder module. Our attention focused on the binding site that forms the central pore between the dimeric structure,

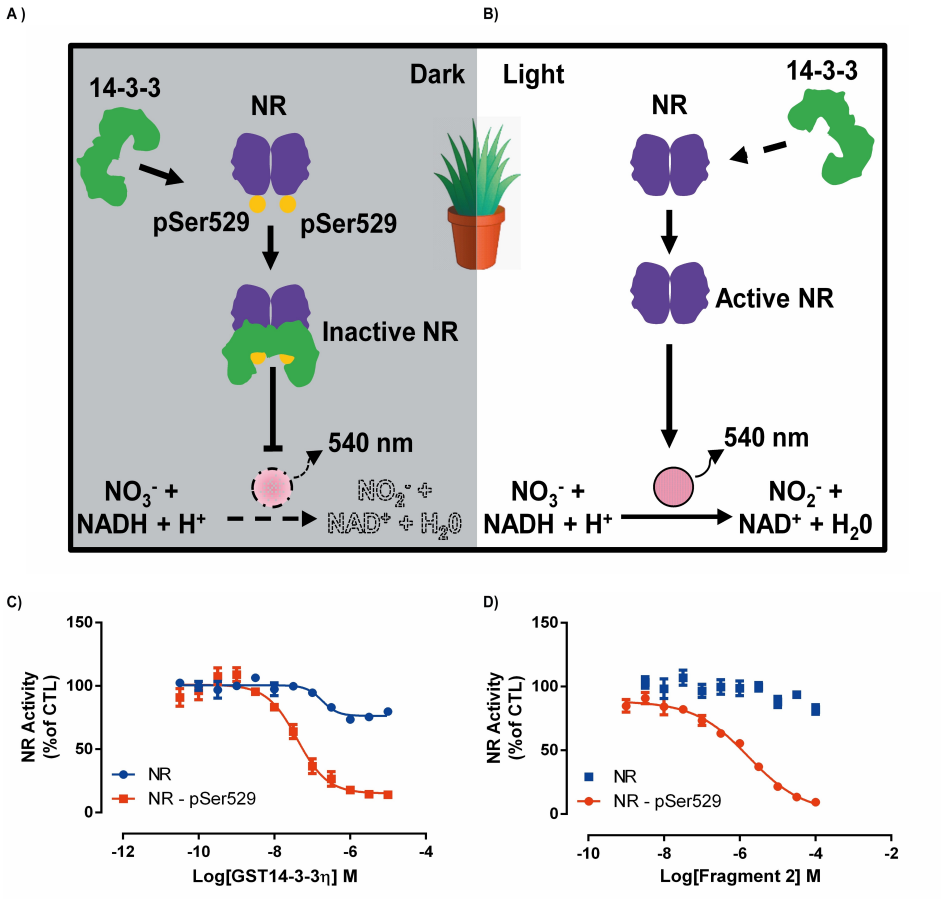

Figure 6. Targeting the nitrate reductase/14-3-3 interaction complex with fragment **2**. A) The NR is phosphorylated in the dark at Ser529 allowing 14-3-3 binding and subsequent inhibition of the enzyme and no nitrite is produced whereas B) in the light the NR remains unphosphorylated and 14-3-3 is unable to bind. Consequently, the NR remains active in the light and reduces nitrate to nitrite. Colorimetric detection of produced nitrite at 540 nm is used as a measure of NR activity. C) 14-3-3 inhibition curves of either the phosphorylated (NR-pS529) or non-phosphorylated nitrate reductase isolated from *Hordeum vulgare*. D) Concentration dependent inhibition of either the phosphorylated (NR-pS529) or non-phosphorylated nitrate reductase by fragment **2** in the presence of a fixed GST14-3-3η concentration. Data are presented as the mean ± SEM of three independent experiments.

which has previously been targeted with small molecules.[33] We specifically focused on the binding site that is aligned by the following listed residues: Chain A: GLN16, ALA17, GLU18, ARG19, TYR20, ASP21, ASP22, ASN51, VAL52, ALA55, ARG56, SER58, SER59, GLU92; Chain B: ALA17(B), GLU18(B), ARG19(B), TYR20(B), ASP21(B), ASP22(B), ASN51(B), VAL52(B), ALA55(B), ARG56(B), SER58(B), SER59(B), VAL62(B), GLU92(B)). A ligand conformation database was prepared that consisted of all stereoisomers, all protonation states and all low energy conformers of fragment **2**. This database was docked using MOE's Dock module in which the post-placement refinement included induced fit, thereby allowing some protein flexibility during optimization. A total of 42 docking solutions passed the default scoring and energy criteria. The best scoring docking solution (mode #1) binds to Asp23 and Glu94(B) (Figure 5A). The third best docking solution binds symmetrically to Asp23 and Asp23(B) (Figure 5B). Other docking solutions either did bind with only one of the quinuclidine rings to the protein, had similar binding modes as #1 and #3 and/or had poor docking scores. These results illustrate that the central pore on the protein dimer interface has the size and shape that can potentially accommodate fragment **2**. More thorough modelling and experimental studies are needed to validate these preliminary studies.

Fragment 2 enhances 14-3-3 mediated inhibition of the nitrate reductase

Finally, we tested whether fragment **2** can modulate the functional role of 14-3-3 in the regulation of a full-length 14-3-3 client enzyme. The enzyme chosen is the well-established 14-3-3 client nitrate reductase (NR) of plants, a 100 kDa enzyme which contains a mode-I 14-3-3 binding motif.[35] NR activity is controlled by reversible post-translational regulation to ensure a rapid response to light/dark changes. In daylight, NR is not phosphorylated (= active) and reduces nitrate (NO_3^-) to nitrite (NO_2^-). At the onset of darkness, NR-Ser529 is rapidly phosphorylated in response to reduced light intensity, creating a 14-3-3 binding site. 14-3-3 binding to the NR inhibits the enzyme (Figure 6A & B).

NR extracts were made from barley leaves grown in the light (NR-Ser529) or in darkness for 2 h (NR-pSer529). The ammonium-sulfate precipitation used to make the extracts removes most of the endogenous 14-3-3 protein. Extracts from dark-grown plants did show NR activity and this activity could be inhibited by adding recombinant GST14-3-3η in a concentration-dependent manner with a pIC_{50} value of 7.4 (Figure 6C). As the residual NR activity at saturating 14-3-3 concentrations was close to zero, we conclude that NR from these dark-grown plants was fully phosphorylated at Ser529. In contrast, NR isolated from light-grown plants was only marginally sensitive to 14-3-3, which indicates that the level of Ser529 phosphorylation was low (Figure 6C).

Next, we investigated the effect of fragment **2** on 14-3-3 mediated inhibition of NR activity in the light- and dark-extracts. The assay was done in the presence of a fixed concentration of GST14-3-3η, using the IC_{50} concentration of GST14-3-3η obtained in Figure 6C. Titration with fragment **2** showed a concentration-dependent inhibition of NR activity in extracts from dark-grown plants with a pIC_{50} of 5.77 (Figure 6D, Table S5). In contrast, NR activity in extracts from light-grown plants was largely insensitive to fragment **2** (Figure 6D). Taken together, these results show that fragment **2** not only enhances the binding of phospho-peptides to 14-3-3, but also potentiates 14-3-3 mediated inhibition of the full-length NR enzyme from dark-grown plants. This effect is clearly 14-3-3 related as the activity of the 14-3-3 insensitive NR was also insensitive to fragment **2**.

Conclusion

Here we report the results of a fragment screen targeting the 14-3-3/ERα interaction complex. Hit fragment **2** (VUF15640) was found to enhance ERα peptide binding to 14-3-3 in the presence of FC-A in a non-competitive manner suggesting that it does not target the canonical FC-A pocket. Mechanistically, fragment **2** does not directly contact the peptide ligand, as is the case with FC-A. Instead, it appears to enhance 14-3-3 dimerization and alters the conformation of 14-3-3 such that it binds peptide ligands with a higher affinity. Finally, the effect of fragment **2** on 14-3-3 interactions was shown to translate into a functional effect as it could enhance the potency of 14-3-3 in a cell-free system inhibiting the NR-Ser529's enzymatic activity. The unusual structure of non-covalent fragment **2** with its high 3D character supports potential merits for three-dimensional fragments. Equally important, fragment **2** may serve as a tool for detailed investigations of the 14-3-3 dimer interface and interactions with various other client proteins.

Acknowledgments

We thank the Amsterdam Institute of Molecular and Life Sciences, Henry Vischer and Saskia Nijmeijer for the experiments carried out at the facilities of the Chemical Biology Platform, and Hans Custers for HRMS measurements. Finally, we would like to thank Reggie Bosma for his insightful comments at all stages of the project.

Conflict of Interest

The authors declare no conflict of interest.

Data Availability Statement

The data that support the findings of this study are available from the corresponding author upon reasonable request.

Keywords: drug discovery · estrogen receptor alpha · fragments · protein-protein interactions · stabilizers

[1] M. R. Arkin, Y. Tang, J. A. Wells, *Chem. Biol.* **2014**, *21*, 1102–1114.
[2] C. S. Harmange Magnani, T. J. Maimone, *Cell Chem. Biol.* **2020**, *27*, 635–637.
[3] L. M. Stevers, E. Sijbesma, M. Botta, C. Mackintosh, T. Obsil, I. Landrieu, Y. Cau, A. J. Wilson, A. Karawajczyk, J. Eickhoff, J. Davis, M. Hann, G. O'Mahony, R. G. Doveston, L. Brunsveld, C. Ottmann, *J. Med. Chem.* **2018**, *61*, 3755–3778.
[4] A. Aitken, *Semin. Cancer Biol.* **2006**, *16*, 162–72.
[5] X. Yang, W. H. Lee, F. Sobott, E. Papagrigoriou, C. V. Robinson, J. G. Grossmann, M. Sundström, D. A. Doyle, J. M. Elkins, *Proc. Natl. Acad. Sci. USA* **2006**, *103*, 17237–17242.
[6] V. Obsilova, T. Obsil, *Int. J. Mol. Sci.* **2020**, *21*, 1–16.
[7] B. Coblitz, M. Wu, S. Shikano, M. Li, *FEBS Lett.* **2006**, *580*, 1531–5.
[8] B. Coblitz, *J. Biol. Chem.* **2005**, *280*, 36263–36272.
[9] F. Madeira, M. Tinti, G. Murugesan, E. Berrett, M. Stafford, R. Toth, C. Cole, C. MacKintosh, G. J. Barton, *Bioinformatics* **2015**, *31*, 2276–2283.
[10] M. Tinti, F. Madeira, G. Murugesan, G. Hoxhaj, R. Toth, C. MacKintosh, *Database* **2014**, *2014*, 1–15.
[11] L. Camoni, S. Visconti, P. Aducci, M. Marra, *Planta* **2019**, *249*, 49–57.
[12] A. Kaplan, A. E. Fournier, *Neural Regen. Res.* **2017**, *12*, 1040–1043.
[13] L. M. Stevers, C. V. Lam, S. F. R. Leysen, F. A. Meijer, D. S. van Scheppingen, R. M. J. M. de Vries, G. W. Carlile, L. G. Milroy, D. Y. Thomas, L. Brunsveld, C. Ottmann, *Proc. Natl. Acad. Sci. USA* **2016**, 133(9), E1152–61.
[14] I. J. De Vries-van Leeuwen, D. Da Costa Pereira, K. D. Flach, S. R. Piersma, C. Haase, D. Bier, Z. Yalcin, R. Michalides, K. A. Feenstra, C. R. Jiménez, T. F. A. De Greef, L. Brunsveld, C. Ottmann, W. Zwart, A. H. De Boer, *Proc. Natl. Acad. Sci. USA* **2013**, *110*, 8894–8899.
[15] P. de Vink, L. Skora, W. Jahnke, L. Brunsveld, K. K. Hallenbeck, S. Leysen, E. Sijbesma, M. R. Arkin, C. Ottmann, *J. Am. Chem. Soc.* **2019**, *141*, 42.
[16] M. Wolter, P. de Vink, J. F. Neves, S. Srdanović, Y. Higuchi, N. Kato, A. Wilson, I. Landrieu, L. Brunsveld, C. Ottmann, *J. Am. Chem. Soc.* **2020**, *142*, 11772–11783.
[17] I. J. P. De Esch, D. A. Erlanson, W. Jahnke, C. N. Johnson, L. Walsh, *J. Med. Chem.* **2022**, *65*, 84–99.
[18] D. A. Erlanson, S. W. Fesik, R. E. Hubbard, W. Jahnke, H. Jhoti, *Nat. Rev. Drug Discovery* **2016**, *15*, 605–619.
[19] E. Sijbesma, B. A. Somsen, G. P. Miley, I. A. Leijten-Van De Gevel, L. Brunsveld, M. R. Arkin, C. Ottmann, *ACS Chem. Biol.* **2020**, *15*, 3143–3148.
[20] F. Centorrino, B. Andlovic, P. Cossar, L. Brunsveld, C. Ottmann, *Curr. Res. Struct. Biol.* **2021**, *4*, 21–28.
[21] X. Guillory, M. Wolter, S. Leysen, J. F. Neves, A. Kuusk, S. Genet, B. Somsen, J. K. Morrow, E. Rivers, L. van Beek, J. Patel, R. Goodnow, H. Schoenherr, N. Fuller, Q. Cao, R. G. Doveston, L. Brunsveld, M. R. Arkin, P. Castaldi, H. Boyd, I. Landrieu, H. Chen, C. Ottmann, *J. Med. Chem.* **2020**, *63*, 6694–6707.
[22] E. Sijbesma, K. K. Hallenbeck, S. Leysen, P. J. De Vink, L. Skóra, W. Jahnke, L. Brunsveld, M. R. Arkin, C. Ottmann, *J. Am. Chem. Soc.* **2019**, *141*, 3524–3531.
[23] P. J. Cossar, M. Wolter, L. Van Dijck, D. Valenti, L. M. Levy, C. Ottmann, L. Brunsveld, *J. Am. Chem. Soc.* **2021**, *143*, 8454–8464.

[24] E. Sijbesma, L. Skora, S. Leysen, L. Brunsveld, U. Koch, P. Nussbaumer, W. Jahnke, C. Ottmann, *Biochemistry* **2017**, *56*, 3972–3982.
[25] M. Molzan, M. Weyand, R. Rose, C. Ottmann, *FEBS J.* **2012**, *279*, 563–571.
[26] D. Valenti, J. F. Neves, F.-X. Cantrelle, S. Hristeva, D. Lentini Santo, T. Obšil, X. Hanoulle, L. M. Levy, D. Tzalis, I. Landrieu, C. Ottmann, *MedChemComm* **2019**, *10*, 1796–1802.
[27] G. E. de Kloe, J. Kool, R. van Elk, J. E. van Muijlwijk-Koezen, A. B. Smit, H. Lingeman, H. Irth, W. M. A. Niessen, I. J. P. de Esch, *MedChemComm* **2011**, *2*, 590–595.
[28] C. de Graaf, H. F. Vischer, G. E. de Kloe, A. J. Kooistra, S. Nijmeijer, M. Kuijer, M. H. P. Verheij, P. J. England, J. E. van Muijlwijk-Koezen, R. Leurs, I. J. P. de Esch, *Drug Discovery Today Technol.* **2013**, *18*, 323–330.
[29] Z. Ji-Hu, T. D. Y. Chung, K. R. Oldenburg, *J. Biomol. Screening* **1999**, *4*, 67–73.
[30] D. J. Hamilton, T. Dekker, H. F. Klein, G. V. Janssen, M. Wijtmans, P. O'Brien, I. J. P. de Esch, *Drug Discovery Today Technol.* **2020**, *38*, 77–90.
[31] S. C. Masters, H. Fu, *J. Biol. Chem.* **2001**, *276*, 45193–45200.
[32] M. Chaudhri, M. Scarabel, A. Aitken, *Biochem. Biophys. Res. Commun.* **2003**, *300*, 679–685.
[33] M. Ehlers, J. N. Grad, S. Mittal, D. Bier, M. Mertel, L. Ohl, M. Bartel, J. Briels, M. Heimann, C. Ottmann, E. Sanchez-Garcia, D. Hoffmann, C. Schmuck, *ChemBioChem* **2018**, *19*, 591–595.
[34] P. Pohl, R. Joshi, O. Petrvalska, T. Obsil, V. Obsilova, *Commun. Biol.* **2021**, *4*, 899.
[35] I. C. Lambeck, K. Fischer-Schrader, D. Niks, J. Roeper, J. H. Chi, R. Hille, G. Schwarz, *J. Biol. Chem.* **2012**, *287*, 4562–4571.

Manuscript received: March 30, 2022
Revised manuscript received: June 28, 2022
Accepted manuscript online: June 29, 2022
Version of record online: July 19, 2022